Low-field NMR Measurement Procedure when SQUID Detection is Used

Longqing Qiu[1,2], Yi Zhang[1], Hans-Joachim Krause[1], Alex I. Braginski[1]
and Andreas Offenhäusser[1]
(1) Institute of Bio- and Nanosystems, Research Center Juelich, D-52425 Juelich, Germany
(2) Pohl Institute of Solid State Physics, Tongji University, Shanghai 200092, P. R. China
e-mail: y.zhang@fz-juelich.de

***Abstract* - In reported low-field nuclear magnetic resonance (NMR) measurements using SQUID (Superconducting Quantum Interference Device) detection, the pre-polarizing magnetic field has been oriented orthogonal to the measuring field, $B_p \perp B_m$. Melton *et al.* were first to analyze the consequences of B_p decay in time after turnoff and showed that this decay should be nonadiabatic. We evaluated the SQUID-based measuring procedure in the light of Melton *et al.* analysis, found good quantitative agreement, and showed that, when the decay time constant is comparable to the precession time of the magnetic moment vector M, the optimum procedure is to orient B_p parallel to B_m and to apply a $\pi/2$ pulse to flip M, similar as in the case of conventional NMR.**

Received June 21, 2008. Accepted June 25, 2008. Reference No. ST35; Category 4.
Paper submitted to a peer-reviewed journal.

Keywords: NMR, SQUID, low field, prepolarization, adiabatical and nonadiabatical.

I. Introduction

In nuclear magnetic resonance (NMR) spectroscopy and magnetic resonance imaging (MRI), the general trend has been to higher measurement fields in order to improve the signal intensity and resolution. In conventional NMR systems, there is only one high magnetic field B in the Tesla (T) range, which acts both as the polarizing and measuring field. A radio frequency (*rf*) pulse near the Larmor frequency f_L, applied perpendicular to B, flips the magnetic moment vector $\boldsymbol{M}$ of the sample to the perpendicular start position (this pulse is called $\pi/2$ pulse). Subsequently, the precession of $\boldsymbol{M}$, which results in the free induction decay (FID) signal, can be detected as function of time.

Recently, a renewed interest in low-field NMR measurements has been motivated by the use of Superconducting Quantum Interference Devices (SQUIDs) as sensitive and frequency-independent magnetic flux detectors [1,2]. However, the measurement arrangement in low field NMR is quite different. Usually, two mutually perpendicular magnetic fields, the stronger pre-polarizing field (B_p) and the weak measurement field

(B_m), are applied. It is assumed that the magnetization $\boldsymbol{M}$ of the sample after turning off B_p is perpendicular to B_m and thus the *ac* pulse is not necessary (the f_L at low B_m is below the radio frequency range, hence we write *ac* instead of *rf*). Such low field NMR measurements are discussed, for example, in [2-6].

The innate limitation of low-field NMR is its low signal-to-noise ratio (SNR). To partially overcome this limitation, an effective and simple method is to increase B_p, as $|\boldsymbol{M}|$ is proportional to B_p. However, a relatively large inductance and a high current are needed to generate higher B_p. Therefore, a longer B_p decay with time constant τ after turnoff is unavoidable. The need to introduce a $\pi/2$ pulse occurs when τ is comparable to the $\boldsymbol{M}$ precession time. For example, McDermott *et al*. increased B_p up to 300 mT [7], and introduced a $\pi/2$-π *ac* pulse sequence after turning off of B_p to detect the spin-echo signal. Similarly, H. C. Yang *et. al.* applied a $\pi/2$ pulse some time after B_p to record the FID signal [8].

Melton *et al*. systematically investigated the B_p decay process by solving the equation of motion $\mathrm{d}\boldsymbol{M}/\mathrm{d}t = \gamma\boldsymbol{M} \times \boldsymbol{B}$, where γ is the gyromagnetic ratio (proton gyromagnetic ratio equals 2.68×10^8 rad/Ts), and analyzing the regimes of "sudden passage" (B_p is reduced quickly and $\boldsymbol{M}$ left behind to precess about B_m) and "adiabatic passage" (B_p is reduced so slowly that $\boldsymbol{M}$ follows it and aligns with B_m without any precession occurring) [9-11]. That work was motivated by Earth's field NMR for oil exploration using a Faraday coil detector. The purpose of our present paper is to evaluate the SQUID-based low-field measuring procedures in the light of Melton *et al*. analysis. Our results suggest that the optimum procedure, when τ is comparable to the $\boldsymbol{M}$ precession time, is to apply B_p parallel to B_m (B_p // B_m) and to apply a $\pi/2$ *ac* pulse to flip $\boldsymbol{M}$, similar as in the case of conventional NMR.

II. Measurement Methods

We performed low-field NMR measurements inside a magnetically shielded room (MSR) using a high-T_c SQUID as the signal detector. The correlations between the B_p decay time constant τ, the period of NMR signal, and its amplitude were investigated quantitatively. The signal outputs were compared with those simulated in [11]. In the case of a loss of signal, a $\pi/2$ *ac* pulse was introduced to recover it. We then compared FID and spin echo signals recorded by using two arrangements, $B_p \perp B_m$ and B_p // B_m.

The nitrogen-cooled *rf* SQUID magnetometer was positioned inside a fiberglass cryostat. This magnetometer is a so-called substrate resonator *rf* SQUID [12]. In MSR, this SQUID exhibits a field resolution of 40 fT $\mathrm{Hz}^{-1/2}$ down to tens of Hz. The sample of 10 ml tap water was placed beneath the bottom of the cryostat finger and at the center of a Helmholtz coil pair (radius: r = 23 cm). This coil current, I_m, generated a homogeneous magnetic field B_m in the sample (B/I = 0.46 mT/A). The distance between the sample center and the SQUID was about 25 mm. A 5-layer solenoid (inductance L_{Bp}=7.2 mH, resistance 11 Ω) surrounded the sample and was used to generate a pulsed polarization field B_p. Its direction was either perpendicular or parallel to B_m and the sensitive direction of SQUID (z-axis). In the measurement configuration of Figure 1(a), only $B_p \perp B_m$ is shown for clarity.

To investigate the influence of the B_p decay on the FID signal, the decay time constant τ was adjusted by a shunt resistance (connected across the B_p solenoid), varied from R = 16.5 Ω to 5 kΩ (5 kΩ was the solenoid's permanent protection resistance) as shown in Figure 1(b). Compared to our previous measurement arrangement [5], two new optional components were added, as schematically shown in Figure 1(a): (i) a coil pair aligned with B_p was used to generate the ac-pulse (B_{ac}); (ii) a gradient field (B_g) was applied to optionally reduce the time constant T_2^* of the free induction decay (FID) signal.

Typically, each measurement started by polarizing the sample in $B_p \approx 10$ mT for t_1 = 10 s controlled by a switch K in Figure 1(b). The SQUID readout electronics was kept in the reset state during the polarizing time. Several milliseconds after B_p was switched off, the sample was left in B_m, which was always kept on. Subsequently, the SQUID was locked to record the signal generated by the precession of $\boldsymbol{M}$ for a preprogrammed measuring time. To obtain the FID signal, a homemade mixer was used to transfer the signal to lower frequency. After careful filtering, the NMR signals were recorded by a Dynamic Signal Analyzer (HP 3562).

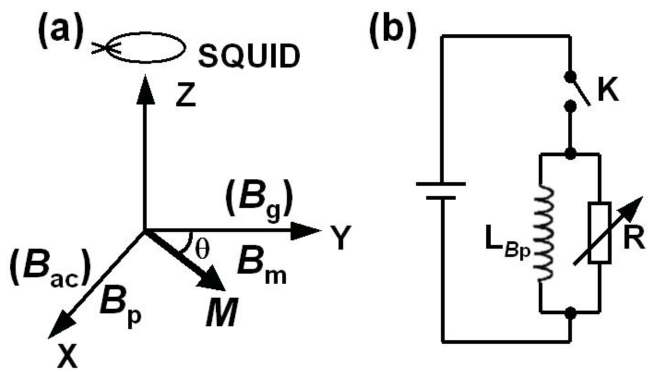

Fig. 1. Measurement configuration and schematic diagram of the pre-polarization field (B_p) circuit. (a) Orientations of measurement field B_m, gradient field B_g, polarization field B_p, ac pulse field B_{ac}, and the sensitive direction of the SQUID. $\boldsymbol{M}$ indicates the orientation of magnetic moment after B_p decayed to zero; and θ is the cone angle between $\boldsymbol{M}$ and B_m. (b) The pre-polarization field circuit: a variable resistor R shunts the coil in order to change the decay time of the polarizing field B_p; the circuit is controlled by an electric switch.

The original intention of arranging B_p perpendicular to B_m has been to simplify the measurement field sequence, and to detect the signal directly after B_p is turned off. However, the magnetic moment $\boldsymbol{M}$ remains in B_p direction only when B_p decays nonadiabatically (sudden passage), which should satisfy the following condition [11]:

$$dB_p/dt >> \gamma B_m^{\;2} \; . \qquad (1)$$

This requirement is easily met for a laboratory SQUID instrumentation operating in ultralow field NMR [4]. However, with B_m or τ increasing, it is more and more difficult to guarantee the sudden passage condition.

III. Results and Discussion

Figure 2 compares FID traces obtained with different τ, adjusted by varying the shunt resistance R. The Larmor frequency of these FID traces is 4.23 kHz.

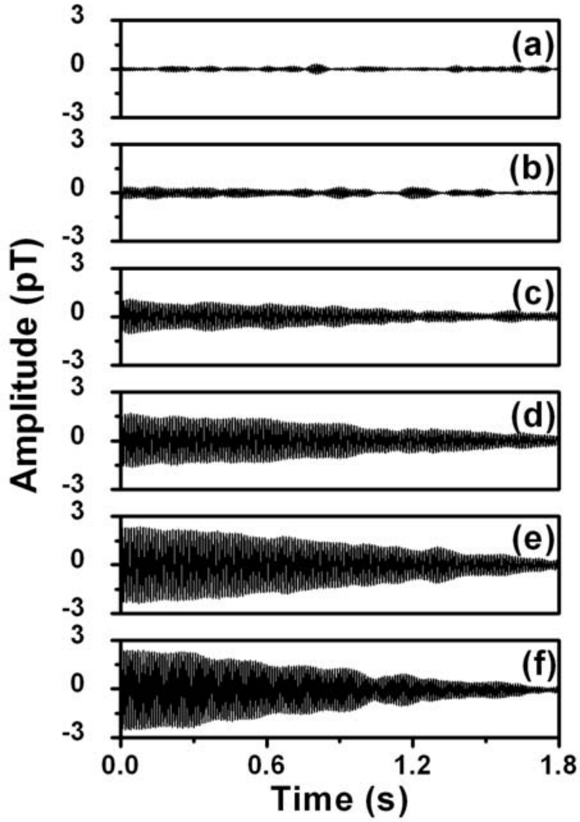

Fig. 2. FID signals of 10 ml tap water with different shunt resistors; f_L = 4.23 kHz. Traces (a) to (f) correspond to shunt resistance R of 47Ω, 100Ω, 220 Ω, 470 Ω, 1000 Ω, and 5000 Ω, respectively. (signals averaged, N = 10)

We note from Figure 2 that traces (e) and (f) have almost the same amplitude, which means the sudden passage condition is satisfied. As R decreases, the FID signal amplitude decreases gradually, and practically disappears when R = 47 Ω. In Figure 2, $\tau = L_{Bp}/R$ (L_{Bp} = 7.2 mH) increases from 1.44 μs to 125 μs when R decreases from 5 kΩ to 47 Ω. Note that after B_p circuit is turned off, the sample is left in two fields: the constant B_m and the exponentially decaying B_p:

$$B_p = B_{p0}\exp(-t/\tau) \ . \tag{2}$$

The decrease of the original amplitude reflects the orientation of the magnetic moment $\boldsymbol{M}$ before each measurement. Only the component $\boldsymbol{M}\sin\theta$ contributes to the signal, with the precession cone angle θ between $\boldsymbol{M}$ and B_m decreasing as τ increases.

In the case of large shunt resistance (say, 1 kΩ or 5 kΩ) resulting in short time constants, B_p decays nonadiabatically, *i.e.*, in a time short compared with the precession period. After B_p decayed off, $\boldsymbol{M}$ still lags behind, is almost on the x-axis and we detect the full signal, as in Figure 2(e) and (f). As the time constant increases, the magnetization follows the resultant field B more and more closely and ends up precessing around B_m in a small cone angle θ. According to [11], the relationship between θ and B_m can be expressed as following formula:

$$\theta = \begin{cases} 2e^{-(\pi/2)\Gamma} & (\Gamma \geq 1) \\ (1-\Gamma)\cdot\pi/2 & (\Gamma \leq 0.4) \end{cases} \tag{3}$$

Here $\Gamma = \omega_m \tau$ is defined as a dimensionless measure of decay time constant.

Figure 3 compared the experimental results from Figure 2 with theoretical values obtained using θ from Eq. [3]. They fit rather well, within an allowable error.

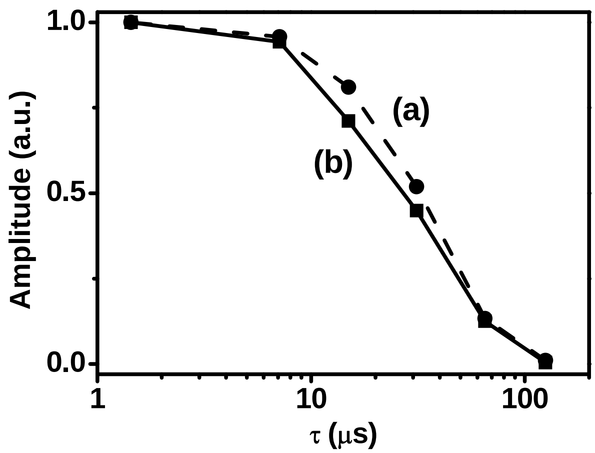

Fig. 3. Theoretical (a) and experimental (b) normalized initial amplitude of FID signals *versus* the decay time constant; f_L = 4.23 kHz.

We investigated also FID signals obtained by varying the shunt resistance at f_L =1.5 kHz and 10 kHz. At 1.5 kHz, the signal disappeared after R was reduced to 16.5 Ω while at 10 kHz no NMR signal remained when the R was less than 220 Ω. These results also agree well with Eq. [3]..

In the case of θ≠90°, the magnetization vector M has a component in y-axis, but it could be rotated back to orthogonal position by a π/2 pulse in x-direction, as shown in Figure 1(a). Figure 4 shows the signal recovery by an *ac* pulse when $B_p \perp B_m$. Several milliseconds after B_p was switched off, we applied a short B_{ac} pulse aligned with B_p, as also indicated in Figure 1(a). The amplitude of this pulse was 4 μT, its frequency was close to f_L = 4.23 kHz, and its duration varied from 236 μs to 6 ms (the number of pulse periods varied from 1 to 26). We plotted the signal amplitude versus the tip angle in radians for three $\tau(R)$.

As seen in Figure 4, at R = 47 Ω, the signal was destroyed totally by the decay of B_p, but the *ac* pulse recovered the signal back to maximum value (at tip angle π/2, 3π/2, 5π/2…, see curve (a). At R = 470 Ω, the signal without the ac-pulse was weaker, but the pulse recalled it fully back (see curve (b)). Curve (c) shows that no ac-pulse is needed when B_p decays quickly enough (nonadiabatically), for ***M*** is still near the x-axis after B_p already decayed.

The results of Figure 4 show (when $B_p \perp B_m$), that the progressing decay of B_p causes the initial orientation of ***M*** to increasingly deviate from θ = π/2, thus adversely affecting the NMR signal. In the case of adiabatical decay (Γ >> 1), ***M*** is reoriented almost along

B_m after B_p decayed to zero, and a π/2 pulse is mandatory to obtain the NMR signal. This observation encouraged us to compare these results with those of the conventional high-field NMR configuration, obtained by rotating the prepolarization coil to align B_p with B_m.

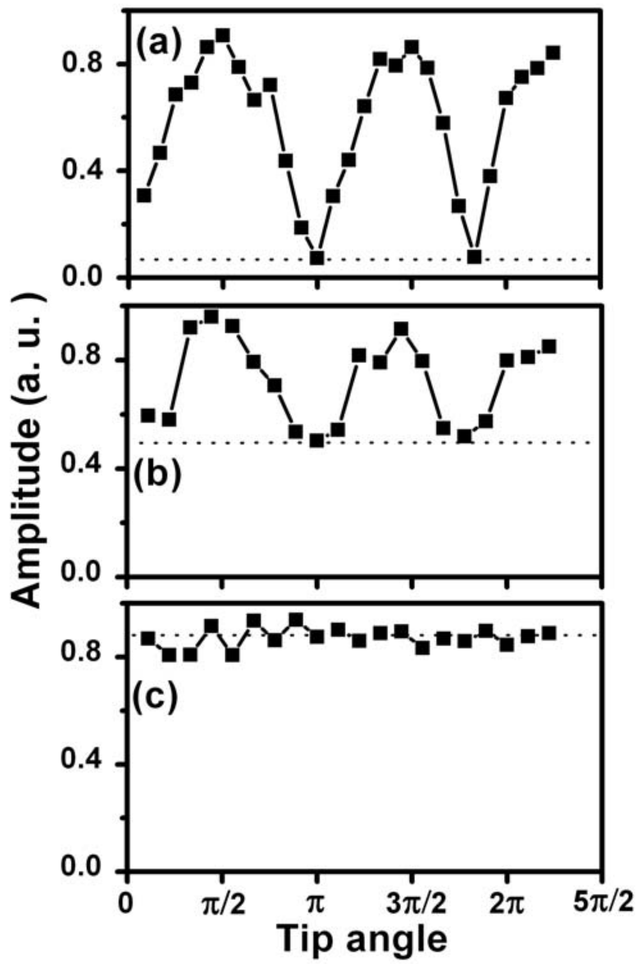

Fig. 4. Signal recovering with an *ac* pulse when f_L = 4.23 kHz, $B_p \perp B_m$. The shunt resistance in curves (a) to (c) is R = 47 Ω, 470 Ω and 5000 Ω, respectively; they illustrate the situations of the NMR signal totally destroyed, partly destroyed and hardly affected. The dotted line in each figure shows the signal level without the *ac* pulse.

Figure 5 compares the FID and the spin-echo signal for the two cases, $B_p \perp B_m$ and B_p // B_m, at the R value of 47 Ω (adiabatic decay). A 30% stronger signal can be detected when B_p // B_m for these two 50 times averaged curves. This is because in this configuration the resulting vector field $\boldsymbol{B}$ would not change its orientation, but only the amplitude. The generated $\boldsymbol{M}$ remains in B_p direction perfectly until flipped by the π/2 *ac* pulse. Therefore, in the case of adiabatic decay, B_p // B_m can avoid any signal loss due to the imperfect fulfilment of the nonadiabatic switching criterion. Further comparisons were also performed at other R values of 470 Ω and 5 kΩ, and results similar to those of Figure 5 were obtained. Only in the case of the typical nonadiabatic decay (R = 5 kΩ, see Figure 4 (c)), the first π/2-pulse applied at 5 ms (see Figure 5) can be saved for obtaining FID signal, when $B_p \perp B_m$.

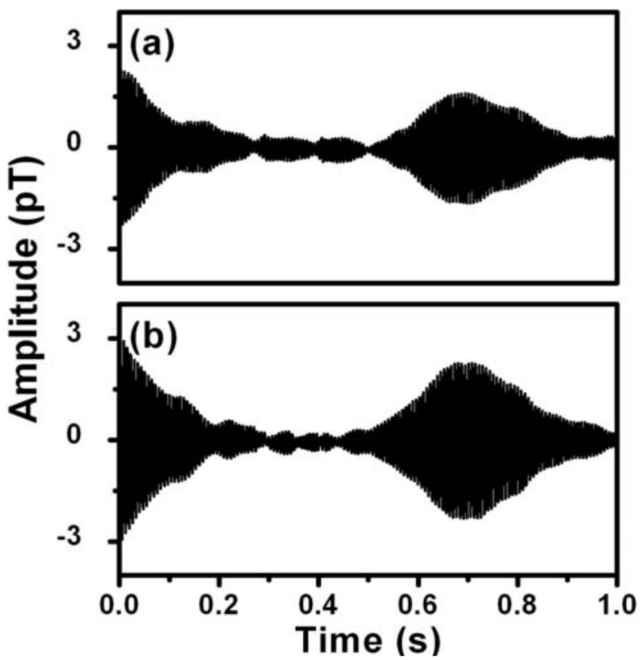

Fig. 5. FID and a spin-echo signal with $B_p \perp B_m$ (a) and $B_p \,//\, B_m$ (b). The $\pi/2$ and π pulse are applied 5 ms and 350 ms after switch-off of B_p. In both cases, the shunt resistance is 47 Ω, and after averaging (N = 50).

IV. Conclusion

In conclusion, using a high-T_c *rf* SQUID magnetometer, we measured NMR signals of liquid proton sample. The transition from nonadiabatic decay to adiabatic decay of B_p was investigated at three typical Larmor frequencies and conformed to the model of Melton *et al.* [9-11]. In cases close to adiabatic decay, a proper ac pulse can recover the signal, at least partially. An improved field configuration is to align B_p with B_m, similar to the conventional NMR field configuration.

Acknowledgments

The authors thank Dr. Bernhard Bluemich of RWTH Aachen, Germany, and Dr. Saburo Tanaka in Toyohashi University of Technology, Japan, for helpful discussions.

References

[1] Ya. Greenberg, "Application of superconducting quantum interference devices to nuclear magnetic resonance", *Rev. Mod. Phys*. **70,** 175 – 222 (1998).

[2] R. McDermott, A. H. Trabesinger, M. Mueck, E. L. Hahn, A. Pines, and J. Clarke, "Liquid-State NMR and Scalar Couplings in Microtesla Magnetic Fields", *Science*, **295** (22), 2247 – 2249 (2002).

[3] A. N. Matlachov, P. L. Volegov, Michelle A. Espy, J. S. George, and R. H. Kraus Jr., "SQUID detected NMR in microtesla magnetic fields", *J. Magn. Reson*. **170,** 1 – 7 (2004).

[4] M. Burghoff, S. Hartwig, L. Trahms, and J. Bernarding, "Nuclear magnetic resonance in the nanotesla range", *Appl. Phys. Lett*. **87**, 054103 (2005) (2005).

[5] Y. Zhang, L. Q. Qiu, H.-J. Krause, S. Hartwig, M. Burghoff, and L. Trahms, "Liquid state nuclear magnetic resonance at low fields using a nitrogen cooled superconducting quantum interference device", *Appl. Phys. Lett*. **90**, 182503(2007).
[6] L. Q. Qiu, Y. Zhang, H.-J. Krause, A. I. Braginski, M. Burghoff, and L. Trahms, "Nuclear magnetic resonance in the earth's magnetic field using a nitrogen-cooled superconducting quantum interference device", *Appl. Phys. Lett*. **91**, 072505 (2007).
[7] R. McDermott, S. K. Lee, B. Haken, A. H. Trabesinger, A. Pines, and J. Clarke, "Microtesla MRI with a superconducting quantum interference device", *PNAS* **101**(21), 7857 – 7861 (2004).
[8] H. C. Yang, S. H. Liao, H.E. Horng, S. L. Kuo, H. H. Chen, and S. Y. Yang, "Enhancement of nuclear magnetic resonance in microtesla magnetic field with prepolarization field detected with high-T_c superconducting quantum interference device", *Appl. Phys. Lett*. **88**, 252505(2006).
[9] B. F. Melton, V. L. Pollak, T. W. Mayes, and B. L. Wlllis, "Condition for Sudden Passage in the Earth's-Field NMR Technique", *J. Magn. Reson*. A **117**, 164 – 170 (1995).
[10] B. F. Melton, and V. L. Pollak, "Optimizing Sudden Passage in the Earth's-Field NMR Technique", *J. Magn. Reson*. A **122**, 42 – 49 (1996).
[11] B. F. Melton, and V. L. Pollak, "Condition for adiabatic passage in the earth's-field NMR technique", *J. Magn. Reson*. **158**, 15 – 22 (2002).
[12] Y. Zhang, J. Schubert and N. Wolters, "Substrate resonator for HTS rf SQUID operation", *Physica* C **372-376**, 282 – 286 (2002).